Fluorination of carbon fibre sizing without mechanical or chemical loss of the fibre

Jean-Charles Agopian, Olivier Teraube, Marc Dubois, Karine Charlet

Fluorination of carbon fibre sizing without mechanical or chemical loss of the fibre

Agopian Jean-Charles*[a], Teraube Olivier[b], Dubois Marc[b], Charlet Karine[a]

*: corresponding author.

[a] Université Clermont Auvergne, CNRS, SIGMA Clermont, Institut Pascal, F-63000 Clermont–Ferrand, France. Mail: {jean-charles.agopian; karine.charlet}@sigma-clermont.fr

[b] Université Clermont Auvergne, CNRS, SIGMA Clermont, ICCF, F-63000 Clermont–Ferrand, France. Mail: {olivier.teraube; marc.dubois}@uca.fr

Abstract: Knowing that carbon fibre reinforced polymers are sensitive to moisture through their interphases, carbon fibres sized with Bisphenol A diglycidyl ether have been fluorinated under a N_2/F_2 atmosphere to confer them a hydrophobic behaviour. Because of differences in reactivity of gaseous F_2 between fibres and sizing, only the latter has been fluorinated, resulting in an interesting covalent fluorine grafting onto the fibres, which has been evidenced by Infrared spectroscopy, ^{19}F Nuclear Magnetic Resonance and Energy-Dispersive X-Ray Spectroscopy. The hydrophobic behaviour has been observed through contact angle measurements. The carbon fibre structure remains unchanged, as seen thanks to X-Ray Diffraction and Raman spectroscopy studies, and tensile tests on single carbon fibres, even if a roughening, evidenced by Scanning Electron Microscope images, occurs. When compared to the bare fibres, the functionalization via sizing fluorination is less energy consuming since the treatment occurs at room temperature.

Keywords: Fluorination; Carbon fibers; Sizing; Hydrophobicity; Epoxy.

1 Introduction

Carbon fibres are high-strength materials, offering the highest specific modulus and strength of all reinforcing fibres. They are widely used as reinforcement materials for composites, notably in aerospace, nuclear and transport industries [1]. One of the largest fields of

applications for carbon fibres is their use as reinforcement with an epoxy matrix [2]. As fibres are chemically stable [3], they are coated with a sizing, which is often a simple epoxy resin, for further use with epoxy matrix [4]. This sizing plays an important role in the fibre/matrix interphase, as its presence controls some of the composite mechanical properties, and allows an optimal fibre/matrix adhesion [5], [6]. In that respect, an efficient fibre/matrix bonding is capital, as it allows to achieve both environmental resistance and maximum static and dynamic mechanical properties [2]. However, this adhesion can be damaged by moisture absorption at the interface, leading to a decrease of the interfacial shear strength [7].

Giving a hydrophobic behaviour to carbon fibres could be a way to avoid or at least to decrease the moisture absorption. Several hydrophobising techniques with conclusive results already exist for carbonaceous materials: electrochemical reduction to covalently modify the carbon fibre surface has caused an increase of the water contact angle from 98° to 130° [8]. Soaking or spraying of fluoroplastics to add a fluoropolymer coating on carbon fibres increased the water contact angle from 52° to 133° [9]. PTFE suspension (5-40 wt%) deposition on carbon fibres followed by a sintering process led to water contact angles above 140° [10]. All these techniques are based on intermolecular interactions through the grafting of non-polar alkyl groups onto the fibre surface. Commonly chosen deposition agents are perfluorinated materials [8].

Another example is the growth of a carbon nanotube forest on microscaled PAN-based carbon fibres, which allowed an increase of the water contact angle from 148° to 169°, such as reported in a review about superhydrophobic carbon-based materials [11]. This highlights the fact that besides the surface chemical structure, its morphology and roughness are responsible for the hydrophobic properties [12]. This nature-inspired nano-roughening is known as the "lotus-leaf" effect, and has already been used on carbonaceous materials, by deposing carbon nanotubes, graphene or carbon nanofibres amongst others [8].

Fluorination is also a well-known way to confer hydrophobic and barrier properties to a wide range of materials, such as polymers [13]–[17], carbon [3], [18]–[20] or wood-based materials [21]–[24]. This is why fluorination of reinforcement fibres sounds like an acceptable way of limiting moisture absorption in order to keep a good interfacial adhesion. It was either possible to fluorinate the bare carbon fibres or sized ones. The first option requires high reaction temperature, between 200 and 500°C according to the crystalline order of the fibres. The higher the structural order, the higher the fluorination temperature. It is to note that the sizing would have burnt if sized fibres were considered for high temperature fluorination [25].

This sizing degradation can lead to a fibre-matrix adhesion decrease, because of the presence of a not-adherent residual perfluorinated sizing [26]. Perfluorination means the saturation of the polymer chains by fluorine atoms (CF_2-CF_2 for the case of a CH_2CH_2 unit). Too high reaction temperature or amount of F_2 gas results in the over-fluorination, i.e. chain disruption with CF_3 groups at their ends and even release of CF_4 and C_2F_6 gases (the polymer burns in F_2 gas as it does in O_2 at high temperature).

Controlled fluorination of the sizing appears then as a promising route, because the adherence of the sizing is maintained and only the outmost surface of the sizing layer is fluorinated. The control of the reactive gas rates, combined with a minute monitoring of the fluorination times, allows this selective fluorination of the sizing. The chosen fluorination apparatus is conventional, but exhibits several advantages:

- As it is based on a dry process, it does not require use and storage of often toxic solvents.
- As sizing fluorination is desired, our gas/solid direct fluorination treatment is faster than some well-known fluorination treatments, such as the utilisation of halogen fluorides [27], or even several gas/solid direct fluorinations which were aiming at fluorinate more severely the carbonaceous materials [18], [28]–[30].
- As sizing fluorination is desired, it does not require high temperatures, unlike some reported plasma fluorinations [31], or numerous fluorination routes aiming at fluorinating the bulk of the carbon fibres [3], [25], [32], [33].
- This fluorination method (with molecular fluorine) is suitable for industrial applications, as already shown in several studies on polymer fluorination [16], [34], [35], unlike gas/solid direct fluorination methods using XeF_2, SF_6, SF_4 or MoF_6 [31].

Moreover, as it will be shown in this article, another benefit of this fluorination route is the possible tailoring of the fibre surface energy through a minute control of the operating conditions. This could be a promising way to optimize the interaction between fluorinated-sized fibres and various polymers, as the interfacial shear strength (IFSS) of a carbon fibres/hydrophobic polymer system has been found to evolve the same way than the γ_s^d/γ_s ratio, where γ_s^d is the dispersive component of the fibre surface energy and γ_s the fibre total surface energy [36]. With mild conditions, fluorination allows a controlled etching of the sizing and then of the dispersive component.

The sizing fluorination can also avoid moisture absorption at the fibre/matrix interface, while still ensuring a good adhesion between the reinforcement and the matrix. In this study, the effects of the fluorination sizing on the carbon fibres will be investigated in order to define the treatment conditions for partial fluorination of the sizing, without huge over-fluorination.

2 Materials and Methods

2.1 Materials

Carbon fibre fabric is a HiMax™ FCIM 313 from Hexcel. With ^{1}H Nuclear Magnetic Resonance (NMR), Attenuated Total Reflectance - Infrared Spectroscopy (ATR-IR) and mass spectroscopy analyses, it has been possible to identify the sizing main pre-polymer as Bisphenol A diglycidyl ether (DGEBA), whose chemical formula is given in Figure 1. DGEBA belongs to the most widely used epoxy-resin family, the diglycidyl ethers [37].

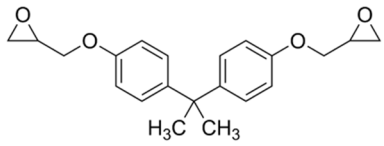

Figure 1 : DGEBA chemical formula

For comparison, fibres were desized by a Soxhlet extraction in acetone for 48h and dried for 24h at 60°C in a Buchi vacuum drier (10^{-3} mbar) [3], [19], [25].

Fluorination samples consisted of 6 carbon fibre bundles which were 4 cm long and dried for 1 hour at 80°C under vacuum (10^{-3} mbar). The glass weft yarns, which ensured the maintaining of the carbon bundles together, were removed before drying.

2.2 Fluorination

Samples were treated under dynamic fluorination. Fluorination apparatus consists of a reactor linked to a pure fluorine gas (F_2, 99.9% purity provided by Solvay) and a nitrogen gas (N_2, 99.999% purity) bottles. A trap containing soda lime (10% NaOH + 80% $Ca(OH)_2$ + 10% KOH) is installed at the reactor output, in order to trap residual F_2 molecules according to these reactions [22]:

$$2\,F_2 + 2H_2O \rightarrow 4HF + O_2$$

$$NaOH + HF \rightarrow NaF + H_2O$$

Carbon bundles were put in a passivated-nickel basket (covered with NiF_2 layer). Then the basket was placed at the centre of the reactor in order to ensure the fluorination reproducibility.

Once the reactor was closed, it was flushed with N_2 at 40 mL/min for 1 hour in order to remove traces of oxygen and moisture. Then the N_2 flow was set at 20 mL/min and the F_2 valve was opened at 20 mL/min too. Several fluorination times were applied: 1, 2.5, 7.5, 10, 15, 20 and 30 min. The fluorine flux valve was switched off afterwards, and the reactor was flushed with N_2 at 40 mL/min for 1 hour, in order to eliminate both the remaining fluorine and side products (HF, F_2O, CF_4 and C_2F_6) in the reactor. Then the carbon fibre bundles were removed from the reactor, while avoiding any HF release, and were dried for 1 hour at 80°C under vacuum (10^{-3} mbar).

2.3 Characterization

Energy-dispersive X-ray spectroscopy (EDX) analyses aim to follow semi-quantitatively the evolution of the fluorine surface mass percentage with the fluorination duration. Carbon, oxygen and nitrogen rates were also measured. These analyses were made with a Bruker Silicon Drift Detector. SEM pictures were taken with a Zeiss Supra 55VP equipped with a Gemini column. Analyses were realised on desized non-fluorinated fibre bundles, sized non-fluorinated fibre bundles and sized fluorinated carbon fibre bundles, which were previously stuck on carbon tape.

In order to evaluate the evolution of the carbon fibre structural organisation depending on the fluorination duration, analyses were realised on a PANalytical X'Pert X-ray diffractometer. The X-ray wavelength was 0.15405 nm (copper K-α). The measure was directly carried out on a fluorinated carbon strand previously taped to a XRD specimen holder. The tape was also analysed in order to remove its diffraction pattern from the carbon fibre diffractogram.

Raman spectrometry gives additional information about the structure of the carbon fibre according to the fluorination duration. Analyses were recorded on a T64000 Jobin Yvon spectrometer equipped with an Olympus confocal microscope with a x50 magnification. The excitation source was a Spectra Physics ionised-argon laser, whose principal line was at 514.5 nm. The laser power was set at 2.3 mW. The measure was directly made on a fluorinated carbon strand. Several zones (at least 3) and for different durations were analysed to check the homogeneity and absence of sample decomposition under the laser beam.

Infrared spectra were recorded on a FT-IR Nicolet 380 spectrophotometer in reflectance mode (diamond ATR-IR). The measure was directly made on a fluorinated carbon strand, with 32 scans per measure.

^{19}F NMR analyses were realised on a 300 MHz Bruker Avance III NMR spectrometer, equipped with a ^{1}H-^{19}F/X 2.5 mm probe, allowing a 30 kHz Magic Angle Spinning (MAS) rate. In order to homogenously fill the probe, fluorinated carbon fibres were cut until their length reached approximatively 1 mm. Each spectrum was acquired with 512 scans at the same received gain for comparison.

Contact angles were measured by putting liquid drops directly on the fluorinated carbon fibre bundles with a micrometric-screw syringe. Several reference liquids were used: water, formamide and diiodomethane. Their polar and dispersive components are reported in the literature [38]~~**Erreur ! Source du renvoi introuvable.**~~**Erreur ! Source du renvoi introuvable.**. The angle measurement was done with the *ImageJ* software.

2.4 Tensile tests on carbon fibres

Tensile tests aim to follow the evolution of the carbon fibre mechanical properties (tensile stress at break, Young's modulus and tensile strain at break) with the fluorination duration. Tests were performed as much as possible in compliance with NF T 25-501-2 standard, at room temperature (around 23°C) on an Instron 5543 tensile testing machine equipped with a 50 N load cell and pneumatic grips. As using an extensometer to get the strain was not possible, the strain has been calculated thanks to the traverse displacement. Tests were carried on fluorinated single carbon fibres, whose diameter has previously been measured with an optical microscope. In order to maintain the fibre in the grips, the fibre was stuck with universal glue to a Kraft-paper frame with a central hole of 10mm. The frame edges were cut before starting the test at a 1 mm/min speed. This method has already been used to realise tensile tests on single flax fibres [39], [40], and is illustrated in Figure 2. For each fluorination duration, at least twenty fibres were tested. For the non-fluorinated (sized and desized) and the 20-minute fluorinated fibres, fifty fibres were tested.

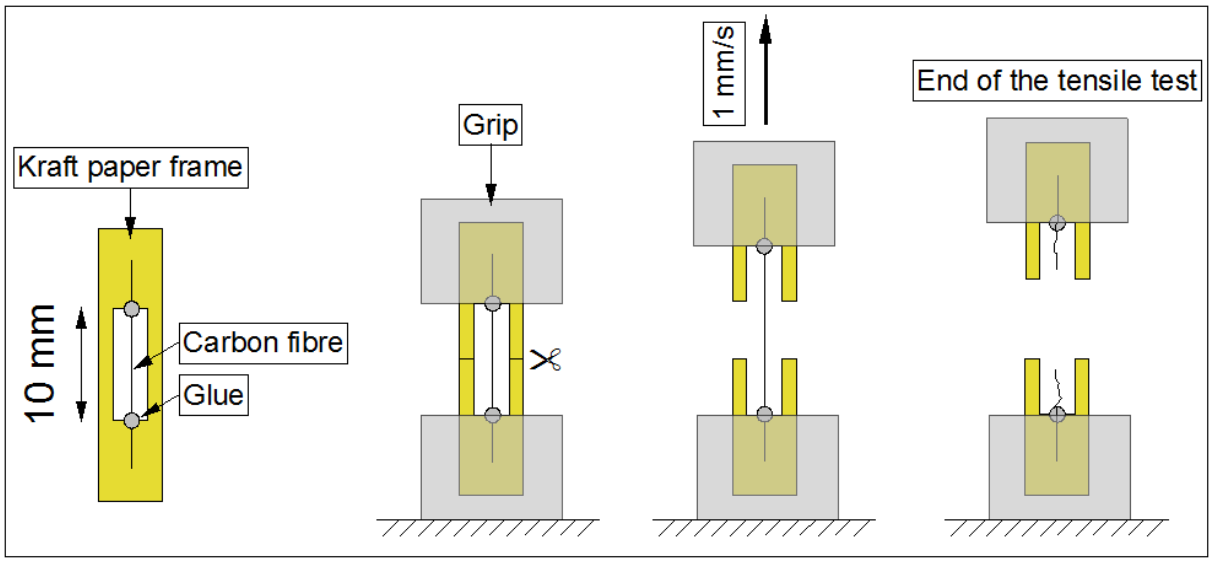

Figure 2 : Tensile test on a carbon fibre

3 Results and Discussion

3.1 Structural and morphological changes

As evidenced by the SEM pictures gathered in Figure 3, fluorination changes the initially smooth fibre surface. Fluorination increases the roughness as the treatment duration increases, with maximal effect for 15 and 20 minutes of fluorination. The roughening occurs along the fibre axis via a probable removal of the external layers of the sized carbon fibres. On the contrary, after 30 minutes of treatment, the fibres seem largely smoother than for previous durations. The roughening effect of the fluorination treatment through decomposition processes is known and may even lead to a complete desizing of the fibres [41]. As discussed in the introduction, this observed roughening could result in a modification of the fibre hydrophobicity. It is to not that the fibres fluorinated for 30 minutes are rougher than the desized ones, which are extremely smooth. The completion of the desizing is then not achieved.

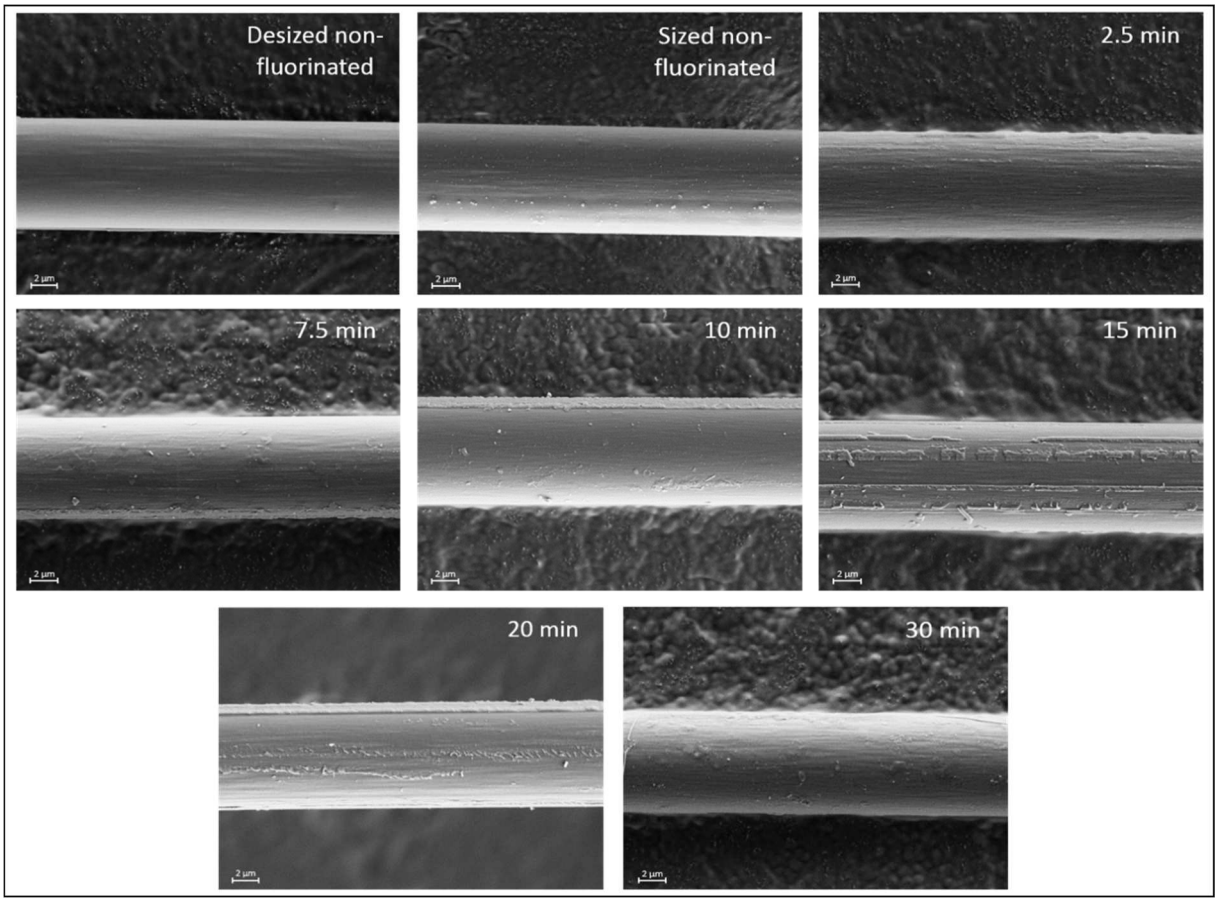

Figure 3: SEM pictures of carbon fibres: desized and non-fluorinated, sized and non-fluorinated, and sized and fluorinated

The evolution of the XRD pattern according to the fluorination duration is given in Figure 4. All peaks belonging to the tape have been already removed from the XRD pattern.

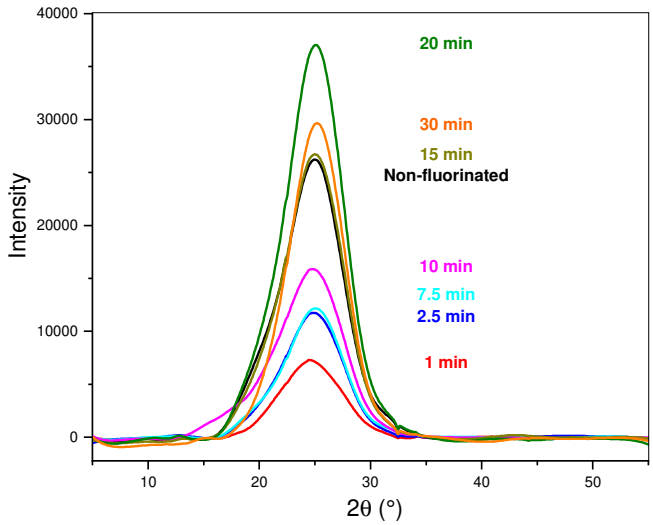

Figure 4: Savitzky-Golay smoothed XRD patterns of fluorinated carbon fibres

The peak at 25.2 ° is assigned to (002) reflection of the graphitic structure [42]. Its broadness gives indication about the poor crystalline order [43]. Further information will be provided by

Raman analyses. The coherence length along the c-axis L_c, calculated using the Scherrer equation [44], and interlayer spacing d_{002} [45] are given in Table 1. Both the interlayer spacing higher than 0.335 Å [46] and L_c around 1.3-1.4 nm [47] evidence a disordered nature. Those parameters appear to be independent of the fluorination duration, evidencing that the fluorination does not structurally affect the carbon fibre bulk.

Table 1: Interlayer spacing and coherence length L_c depending on the fluorination duration

Fluorination duration (min)	0	1	2.5	7.5	10	15	20	30
Interlayer spacing d_{002} (nm)	0.355	0.356	0.352	0.352	0.357	0.353	0.352	0.350
Coherence length L_c (nm)	1.4	1.3	1.4	1.4	1.3	1.3	1.4	1.4

The change of the Raman spectra depending on the fluorination duration confirms this fact (Figure 5). Regardless of the fluorination duration, the spectra exhibit similar shapes.

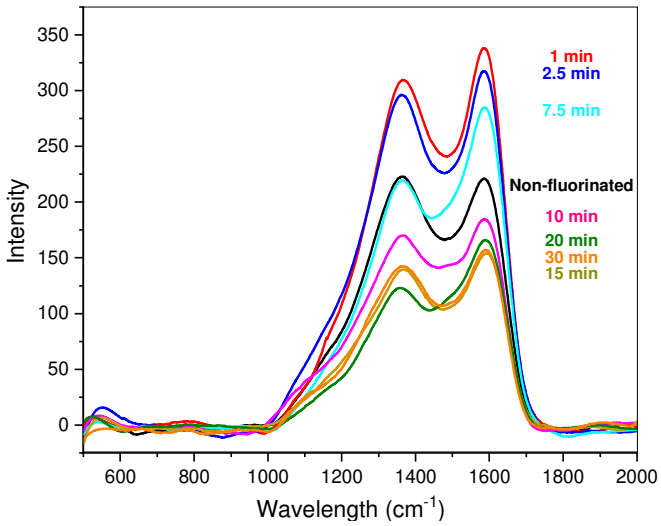

Figure 5: Savitzky-Golay smoothed Raman spectra of fluorinated carbon fibres

The peak at 1585 cm^{-1} (G-band) is assigned to the graphitic structure of carbon, while the peak at 1367 cm^{-1} (D-band) is attributed to the disordered finite-size microcrystalline carbon. Both bands can be attributed to graphitic sp^2 bonded carbon [48]. The intensity of the D-band confirms that the chosen fibres are poorly organised. The coherence length parallel to the graphene sheets L_a, is estimated from the intensity ratio I_D/I_G according to the Tuinstra & Koenig relation [49], [50]:

$$\frac{I_D}{I_G} = \frac{C(\lambda)}{L_a}$$

where I_D and I_G are the intensities of the D-band and the G-band, λ the laser wavelength, and $C(\lambda)$ can be written [51]:

$$\begin{cases} C(\lambda) = C_0 + \lambda C_1 \\ C_0 = -12.6\ nm \\ C_1 = 0.033 \end{cases}$$

Knowing the disordered nature of the carbon fibres, the Ferrari's relation can be considered too; for L_a lower than 2 nm and when the G-band shifts from 1600 to 1510 cm^{-1}, the Tuinstra & Koenig's relation is not adapted anymore [52], [53], because the carbon material is going from nanocrystalline graphite to sp^2 amorphous carbons [54]. In this case, the Ferrari relation is as follows [52]:

$$\begin{cases} \dfrac{I_D}{I_G} = C'(\lambda) L_a^2 \\ C'(544\ nm) = 0.0055 \end{cases}$$

The results obtained on fluorinated carbon fibres are given in Table 2. Given that the G-band of the carbon fibres is located at 1585 cm^{-1} and that L_a is slightly higher than 2 nm, we consider that the Tuinstra & Koenig's relation is still suitable.

Table 2: I_D/I_G ratio and coherence length L_a depending on the fluorination duration

Fluorination duration (min)	0	1	2.5	7.5	10	15	20	30
$\boldsymbol{I_D/I_G}$	1.26	1.13	1.18	0.96	1.24	1.11	0.90	1.12
$\boldsymbol{L_a}$ **(nm)**	3.5	3.9	3.7	4.5	3.5	3.9	4.8	3.9

Both coherence lengths L_a (around 4 nm) and L_c (around 1.2 nm) confirm that the fibres are disorganised [47] with I_D/I_G close to 1. Moreover, the structural parameters are not evolving with the fluorination duration, which highlights that the crystallinity of the carbon fibre is not modified by the fluorination process.

3.2 Tensile tests on single carbon fibres

The carbon fibre diameters, measured using an optical microscope, are given in Table 3.

Table 3: Fibre diameter depending on the fluorination duration

Fluorination duration (min)	0	1	2.5	7.5	10	15	20	30

Average diameter (µm)	7.0 ± 0.1	7.0 ± 0.2	7.2 ± 0.5	7.1 ± 0.4	7.0 ± 0.2	7.0 ± 0.2	7.0 ± 0.2	7.1 ± 0.3

The diameter does not evolve with the applied fluorination treatment, meaning that the fluorination treatment only slightly etched the fibre surface; the SEM images evidence that the fibres have been changed by the fluorination, but the diameter remains constant. The treatment was mild enough to avoid the diffusion of the fluorine atoms in the fibre bulk, which would lead to a diameter increase [29].

The results of the tensile tests are summarised in Table 4. Although the carbon fibre are synthetic fibres (by opposition with natural fibres with high variability) and the relatively high number of samples by fluorination duration, standard deviations are very high for all the mechanical values. Given the errors, average values appear to be independent of the fluorination duration. This scattering between the values could be due to surface flaws leading to early breakings [20]. However, as scattering was already important for non-fluorinated fibres, it cannot be attributed to pit holes or additional surface damages caused by a strong fluorination treatment, as previously reported in literature [3], but rather to the fibre initial structure. Moreover, as the mechanical values remain stable, it means that the fibre is not degraded by the fluorination treatment in accordance with physicochemical characterization.

Table 4: Evolution of the mechanical properties with the fluorination duration

Fluorination duration (min)	0 (desized)	0 (sized)	1	2.5	7.5	10	15	20	30
Stress at break (MPa)	4200 ± 940	4030 ± 930	3800 ± 1100	4340 ± 850	4130 ± 960	4200 ± 860	4000 ± 900	4250 ± 1020	4210 ± 860
Young's Modulus (GPa)	223 ± 20	198 ± 20	215 ± 24	209 ± 26	203 ± 25	205 ± 24	221 ± 27	216 ± 31	192 ± 24
Strain at break (%)	1.6 ± 0.4	1.7 ± 0.4	1.5 ± 0.4	1.7 ± 0.3	1.7 ± 0.4	1.7 ± 0.3	1.5 ± 0.3	1.7 ± 0.4	1.8 ± 0.4

Considering the fibre structure and mechanical properties, the fluorination conditions (room temperature and dilution with N_2) are mild enough to avoid high fibre degradation and even fluorination.

3.3 Sizing evolution

Epoxy resins have been shown to be quite sensitive to fluorination. As a matter of fact, the treatment duration to form a fluorinated layer thick of 1 µm at room temperature for a fluorine pressure of 100 mbar is close to 50 min for an epoxy film. On the other hand, forming the same thickness of the fluorinated layer on polypropylene or Low Density Polyethylene (LDPE) films requires respectively 300 min and 750 min in the same conditions [16]. The changes of the contact angle with water depending on the fluorination duration are given in Figure 6a. As it can be seen on Figure 6b, contact angle is increasing with the fluorination duration, as expected due to the usual hydrophobic behaviour of fluorinated surfaces [55]. The maximal contact angle of 105° was obtained with the sized fibre fluorinated for 20 min: the fibre acquires a hydrophobic behaviour thanks to the sizing fluorination, with a contact angle close to the polytetrafluoroethylene (PTFE) one (reported in between 108° and 114° [56]). However, several studies about commercial polymers reported a decrease of the water contact angle for short fluorination durations, followed by a return close to the initial values. This behaviour has been reported for polyethylene [57] and polypropylene [58], and could be due to the oxidation accompanying the fluorination, or to the dipole moments of the partially fluorinated polar "molecules" [58].

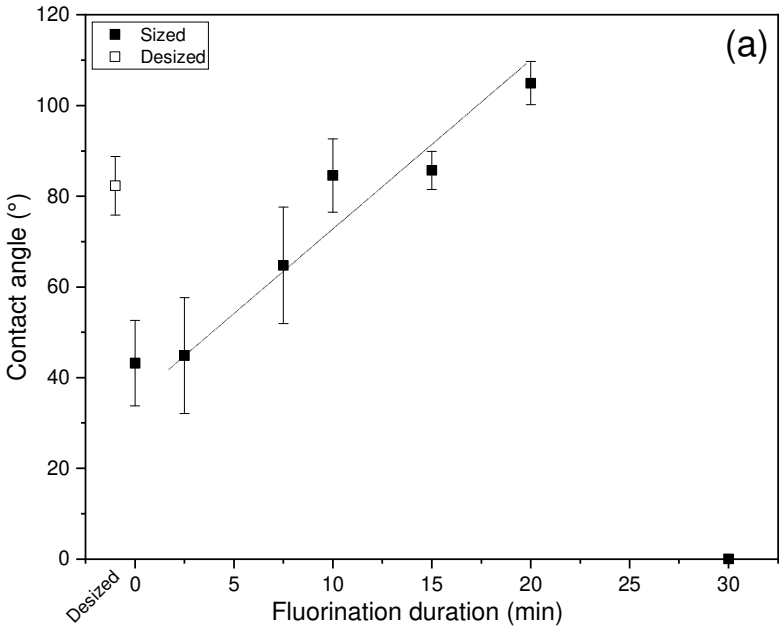

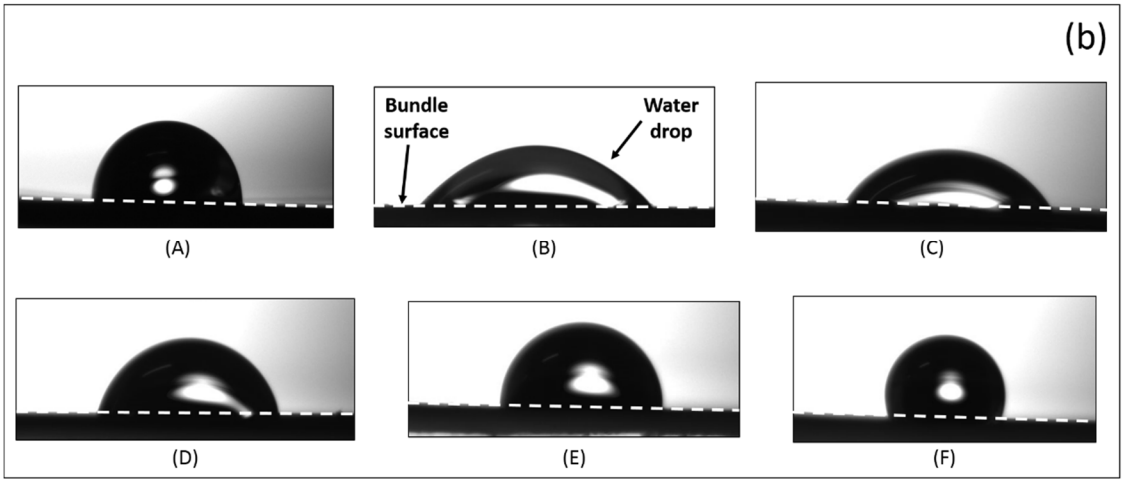

Figure 6: Measured contact angle with water depending on the fluorination duration (a) and pictures of these contact angles on carbon fibres (b) : desized and non fluorinated (A), sized and non fluorinated (B), fluorinated 2.5 min (C), 7.5 min (D), 15 min (E) and 20 min (F)

For the longer treatment time, the water contact angle cannot be measured because the drop is readily absorbed. It is worth noting that the hydrophobic character after 10 and 15 min fluorination is similar to desized fibres and even higher for longer duration.

Contact angles have been measured using three different reference liquids, which enables the polar and dispersive parts of the surface energy to be determined, thanks to the Owens and Wendt's equations [59], [60]:

$$\begin{cases} \gamma_{sl} = \gamma_s + \gamma_l - 2\sqrt{\gamma_s^d \gamma_l^d} - 2\sqrt{\gamma_s^p \gamma_l^p} \\ \gamma_s = \gamma_{sl} + \gamma_l \cos\theta \\ \gamma_l(1 + \cos\theta) = 2\sqrt{\gamma_s^d \gamma_l^d} - 2\sqrt{\gamma_s^p \gamma_l^p} \\ \gamma_s = \gamma_s^d + \gamma_s^p \end{cases}$$

where θ is the contact angle of liquid on solid surface, γ_{sl} the interfacial energy between solid and liquid, and γ the surface energy. The subscripts *s* and *l* and the superscripts *p* and *d* respectively stand for solid, liquid, polar component and dispersive component.

The obtained polar and dispersive components of fluorinated carbon fibres are given in Figure 7. Until 20 minutes, the fluorination tends to reduce the fibre polarity, while the dispersive part stays relatively stable.

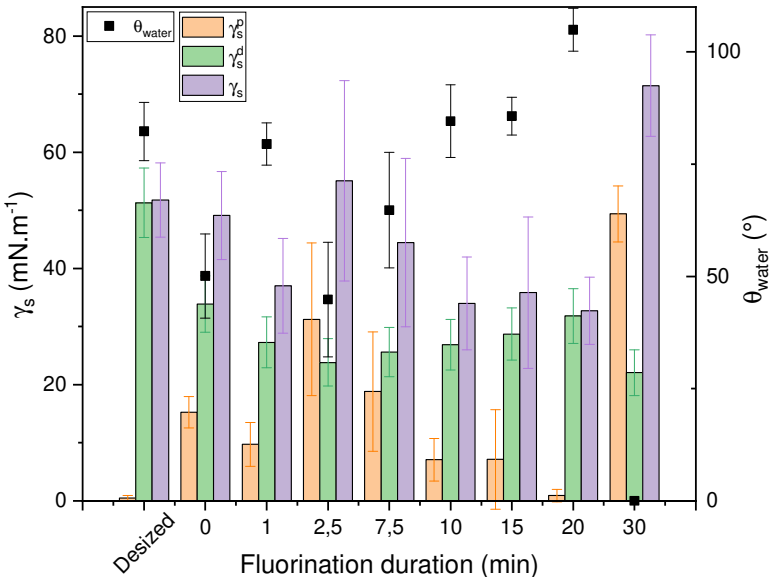

Figure 7: Polar and dispersive components of sized non-fluorinated fibres and sized fluorinated fibres

The γ_s^d/γ_s ratio depends on the fluorination duration for sized fibres (Table 5). It increases until 20 minutes of fluorination, and then drops for a 30-minute treatment. According to a previous study on the relation between surface energies of carbon fibres and IFSS [36], the IFSS between carbon fibres and epoxy should be maximal for a 20-minute fluorination, as the γ_s^d/γ_s ratio is maximal for this duration. It should be noted that the desizing of the fibres led to a highly dispersive surface, with a total surface energy close to the sized non-fluorinated ones.

Table 5: Evolution of the γ_s^d/γ_s ratio with the fluorination duration

Fluorination duration (min)	0, desized	0, sized	2.5	7.5	10	15	20	30
γ_s^d/γ_s	0.99	0.69	0.43	0.58	0.79	0.80	0.97	0.31

The infrared spectra of the non-fluorinated fibres are shown in Figure 8a with vibration band assignment in Table 6. The “reference” bands are the ones commonly used to follow the evolution of DGEBA chemical change during a treatment, such as curing [61].

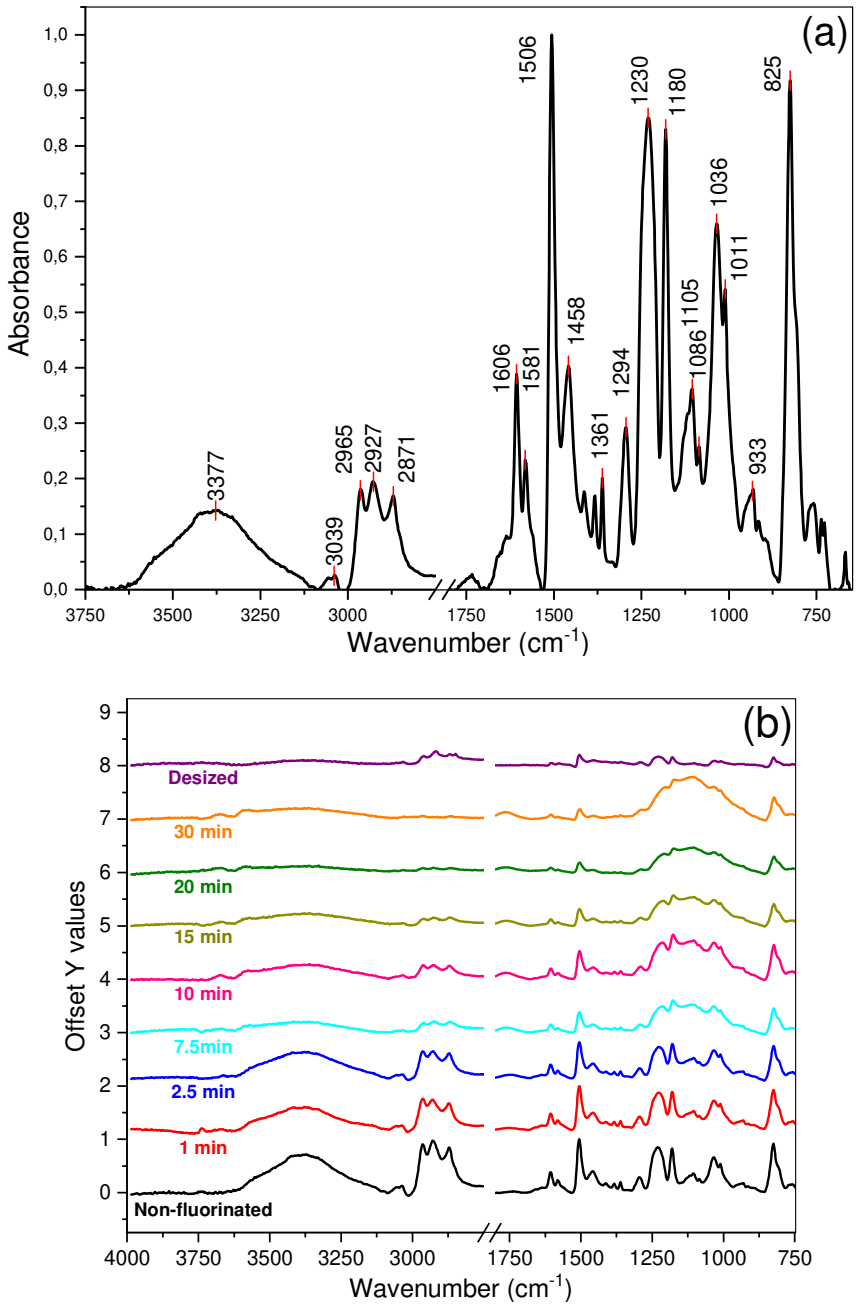

Figure 8: Infrared spectra of non-fluorinated (a) and fluorinated carbon fibres (b)

Table 6: Characteristic bands of DGEBA in the mid IR

Band (cm^{-1})	**Assignment**
≈ 3400	O-H stretching [62]
3039	Stretching of C-H of the oxirane ring [62]
2965 - 2871	C-H stretching of CH_2 and CH aromatic and aliphatic [62]
1606	C=C stretching of aromatic rings [62], reference band [61]
1581	C=C stretching of aromatic rings [63]
1506	C-C stretching of aromatic rings [62], reference band [61]
1458	CH_2 and asymmetric CH_3 stretching + C=C bending [64]
1361	Symmetric CH_3 stretching [64]
1294	C-O-C stretching of aryl alkyl ethers [65]
1230	C-O-C stretching of aryl alkyl ethers [65]

1180	C-O-C stretching of aryl alkyl ethers [65], reference band [28]
1105	C-OH bending of alcohols [66]
1086	C-OH bending of alcohols [66]
1036	C-O-C stretching of ethers [62]
1011	C-OH bending of alcohols [67]
933	C-O stretching of oxirane group [62], reference band [61]
825	C-O-C stretching of oxirane group [62] or H-phenyl [63], reference band [28]

The evolution of the infrared spectra depending on the fluorination duration is given in Figure 8b, where the plot has an x5 offset between 4000 and 2750 cm^{-1}.

It can be seen on Figure 8b that the intensity of the bands at 2965 - 2871 cm^{-1}, 1609 cm^{-1} and 825 cm^{-1} tends do decrease with the fluorination duration, suggesting that the sizing chemical groups responsible for these bands are modified or disappearing. The decrease in the intensities of these bands, used as markers for the presence of sizing, has been plotted in Figure 9a: the three chosen reference bands follow the same trend. Another remarkable band is disappearing with increasing fluorination time: the C-OH vibration band at 3375 cm^{-1} band, meaning that C-OH bonds are replaced by C-F bonds, as already seen in literature [34]. This phenomenon could be responsible for the hydrophobic behaviour of fluorinated fibres, as -OH bonds are interacting with water thanks to hydrogen bonding, while fluorinated surfaces are known for their hydrophobic behaviour [22].

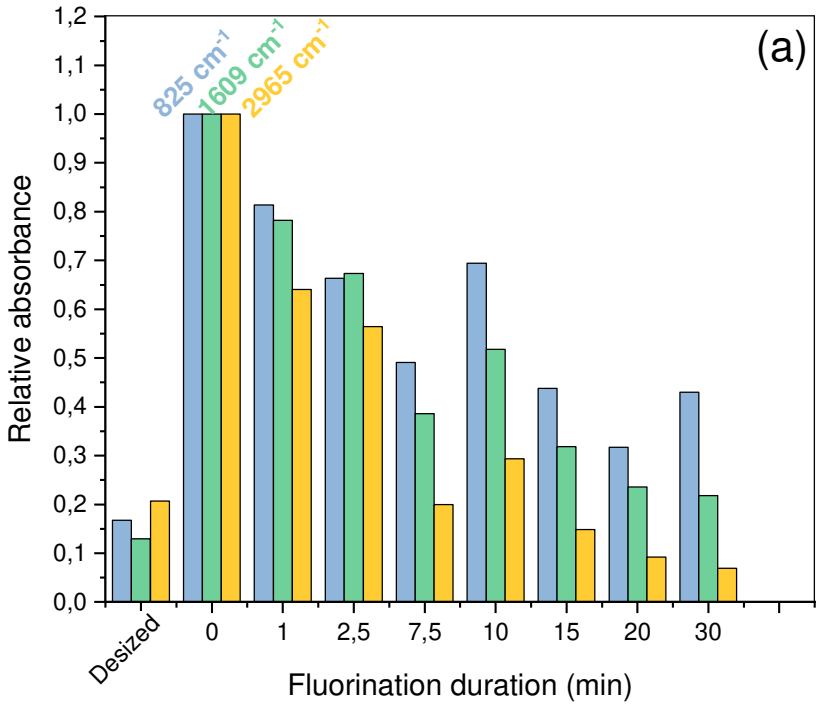

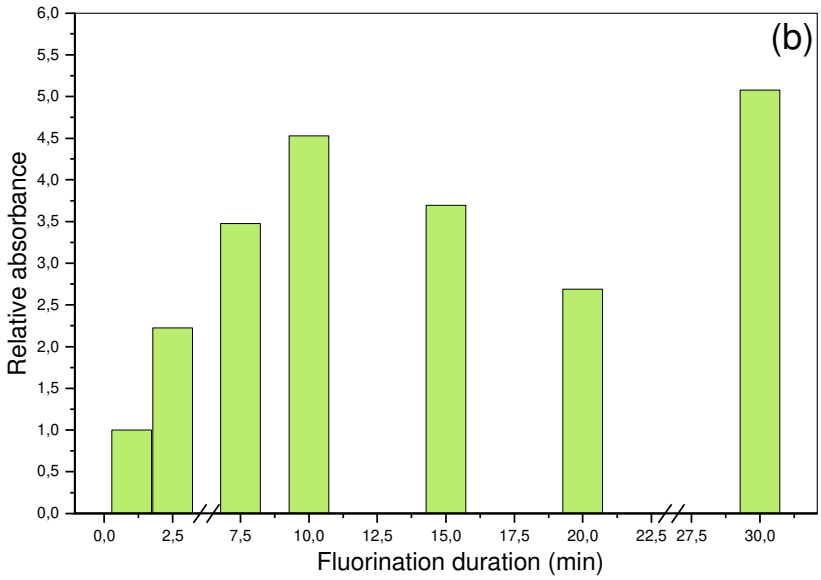

Figure 9: (a) Relative band absorbance compared to the band of non-fluorinated sized carbon fibres; (b) Relative band absorbance of the 1760 cm^{-1} band compared to the 1760 cm^{-1} band of 1 min fluorinated carbon fibres

As already reported for LDPE [68], fluorination leads to a replacement of hydrogen atoms by fluorine atoms, in accordance with the decrease of the 2965 - 2871 cm^{-1} bands and the increase of the 1250 - 1000 cm^{-1} massif. Moreover, for the case of polystyrene [34], all the C-H bonds and CH_2 groups were replaced by C-F and CF_2, and the C=C aromatic bonds were saturated with fluorine [14]–[17], [34], [35], [68]. This could explain the decrease of the 825 cm^{-1} and 1609 cm^{-1} bands with the fluorination duration. On the other hand, the intensities of the 1760 cm^{-1} band and of the 1250 - 1000 cm^{-1} massif increase. The 1760 cm^{-1} band has been assigned to the hydrolysis of -COF groups in -COOH, due to the following post-fluorination reaction with ambient-atmosphere H_2O [57]:

$$-COF + -H_2O \rightarrow -COOH + -HF$$

As it can be seen in Figure 9b, the relative absorbance of the 1760 cm^{-1} band evolves irregularly. Except for the 30-min fluorination, this evolution can highlight two antagonist phenomena that could be in competition during the fluorination treatment: the longer the fluorination treatment lasts, the more -COF groups will be created and hydrolysed in -COOH, leading to a 1760 cm^{-1} intense band. On the other hand, as the sizing begins to be saturated with fluorine atoms, chain scissions can occur to form $-CF_3$, or gaseous CF_4 and C_2F_6, leading to a decreasing number of -COF groups; the relative content of fluorinated sizing decreases. Fluorination and decomposition compete at any duration and the second is dominant for longer treatments. It can be remembered here that the weakest water contact angle is obtained

for the fibres fluorinated for 30 min, which exhibit the highest intensity for 1760 cm^{-1} band. This band was attributed to -COOH group: even if the sizing is degraded, this hydrophilic group can facilitate the drop absorption; if the sizing was only degraded without these -COOH groups, the contact angle would be as high as the desized-fibre one, which is obviously not the case.

The 1250 - 1000 cm^{-1} massif consists of several superimposed bands, which are due to the absorption of C-F_x groups [57]. This massif is growing with increasing the fluorination duration, that is in accordance with substitution of hydrogen and saturation of aromatic C=C by fluorine as previously explained. In the 1250 - 1000 cm^{-1} area, as some fluorinated group bands are growing while some sizing bands are decreasing, the deconvolution is difficult. The comparison between intensity ratios of selected bands was rather chosen. The chosen fluorinated group band was at 1230 cm^{-1}, while the sizing one was at 1100 cm^{-1} band (Figure 10). The ratio can be extrapolated with a power function $y = ax^b$ with $b < 1$, which describes a slow increase of the I_{1100}/ I_{1230} ratio with time. This low value of b can be explained by two facts: i) the fluorination slows down with time as the polymer becomes saturated with fluorine, i.e. perfluorinated (slow increasing of I_{1100}), and ii) fluorinated sizing might even be degraded by additional incoming fluorine, leading to hyperfluorination and chain scissions (small decreasing of I_{1100}).

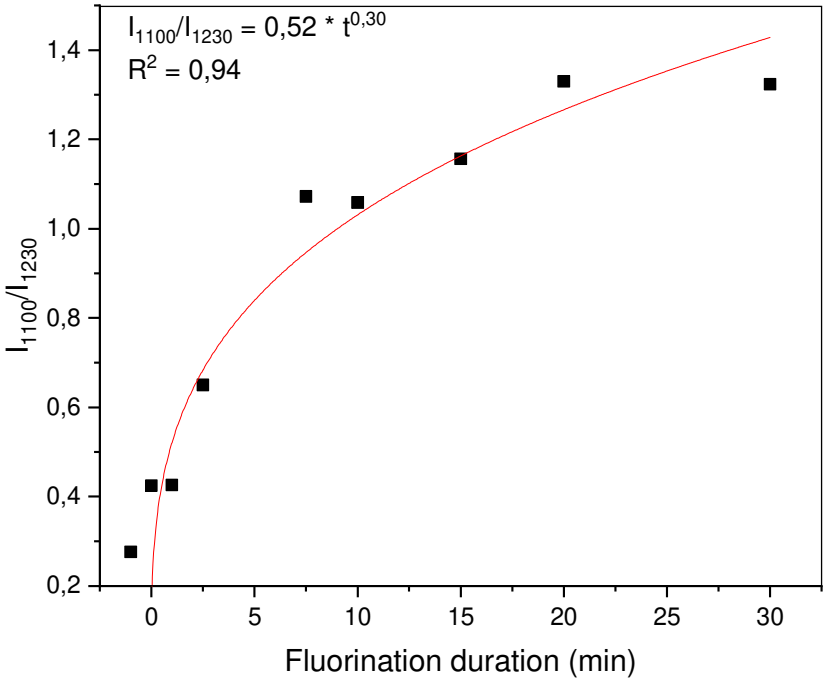

Figure 10: Evolution of the I_{1100}/ I_{1230} ratio with the fluorination treatment duration

The ^{19}F MAS NMR spectra of the fluorinated fibres is shown in Figure 11a. The three broad lines correspond to superimposed components that involve different groups: >CHF (or C-F), $>CF_2$ and $-CF_3$ [22], carbon atoms being all with sp^3 hybridization. The covalent grafting of fluorine on the sizing is confirmed and NMR give additional information about the relative content of CHF, CF_2 and CF_3 (contrary to IR spectroscopy).

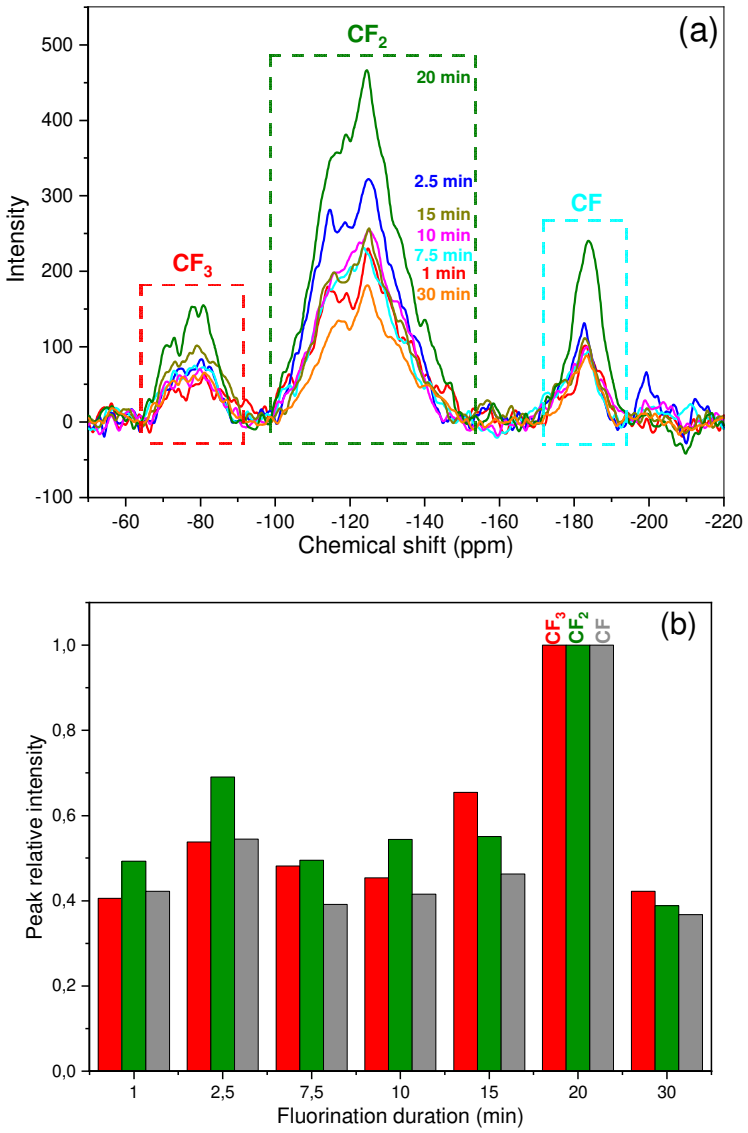

Figure 11: (a) Evolution of the ^{19}F NMR spectra with the fluorination duration, (b) relative band intensity depending on the fluorination duration

In order to ease the comparison between the different NMR spectra, the relative band intensities depending on the fluorination duration were plotted in Figure 11b. It can be seen that the fluorine content slowly increase until the 20-min treatment, before falling down for the 30-min fluorination. The only explanation is the over-fluorination of CF_2 and CF_3 groups into gaseous CF_4 and/or C_2F_6, leading to an average decrease of the band intensities by sizing

degradation. The most fluorinated fibre is also the more hydrophobic with a water contact angle of 105°, which confirms the hydrophobic behaviour that can be brought by fluorine onto sizing.

Surprisingly, the S_{CF_3}/S_{CF}, S_{CF_3}/S_{CF} and S_{CF_3}/S_{CF_2}, ratios, where S is the integrated area of the line, do not change drastically with increasing fluorination time, as presented in Table 7.

Table 7: Evolution of the S_{CF_3}/S_{CF}, S_{CF_3}/S_{CF} and S_{CF_3}/S_{CF_2}, ratios with the fluorination duration

Fluorination duration (min)	1	2.5	7.5	10	15	20	30
S_{CF3}/S_{CF2}	3.95	5.28	4.84	5.27	3.23	4.54	3.98
S_{CF3}/S_{CF}	1.3	1.08	0.99	0.87	1.52	0.9	1.19
S_{CF2}/S_{CF}	5.12	5.71	4.78	4.56	4.89	4.1	4.74

It seems that the chemical composition of the fluorinated layer is close whatever the reaction duration, contrary to other polymers. The conventional mechanism is a progressive increase of CF_3 components for polyethylene [13] or highly reactive compounds such as wood species [22]–[24], [69]. Because of the permanent competition between covalent grafting of F atoms and decomposition into CF_4, C_2F_6, F_2O, HF gases, a layer with nearly constant thickness and chemical composition could be formed. Figure 12 summarizes the most probable mechanism.

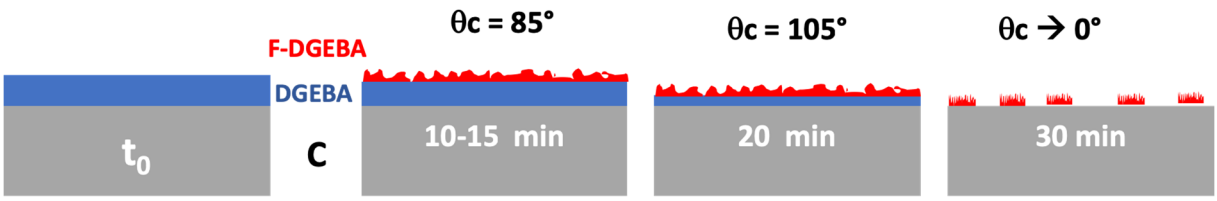

Figure 12: Fluorination scheme of sized fibres (F-DGEBA is fluorinated sizing, θ_c the water contact angle)

The mass percentage of fluorine detected at the fibre surface with increasing fluorination duration is plotted in Figure 13.Values are weak because initial sizing is usually only 0.5 to 2 wt% of the {carbon fibre + sizing} system [70]. Even perfluorinated, the sizing cannot contribute much more to the fluorine content. Overall, it appears that the surface fluorine

content increases with the fluorination duration, until reaching a maximum for the 20 min treatment. This observation is in good agreement with the ^{19}F NMR and ATR-IR data. It is to note the dispersion of the data for each fluorination time.

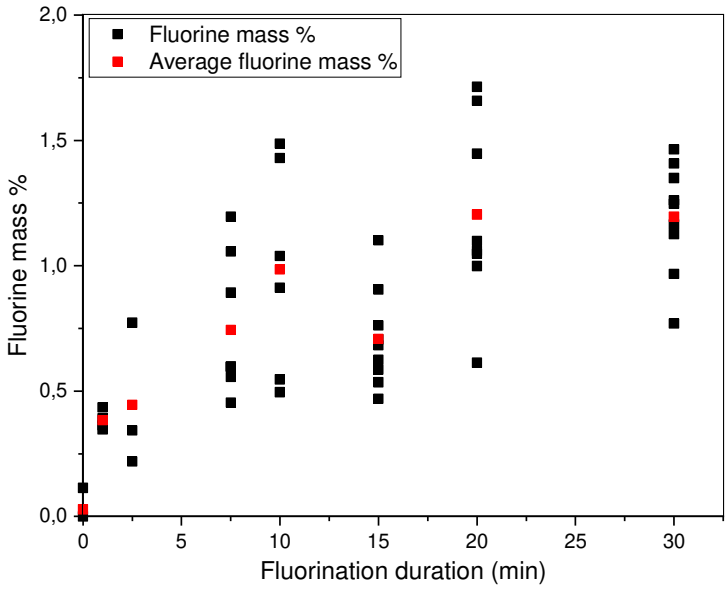

Figure 13: Fluorine mass % evolution with the fluorination treatment duration

To conclude this section about the sizing changes with the fluorination treatment, it appears obvious that the fluorination results in a covalent grafting of fluorine on DGEBA. All ATR-IR, ^{19}F NMR and EDX data converge to this conclusion. Such a grafting occurs via the conversion of C-H (both aliphatic and aromatic), C-O and probably opening of epoxy COC cycle, which are responsible of hydrophilic character of the sizing. A hydrophobic behaviour of the carbon fibre is then achieved as evidenced through the water contact angle changes. The optimal fluorination duration appears to be 20 minutes, because of the high content of grafted fluorine and the fibres are still probably covered by sizing. The maximal contact angle is then found, almost as high as the PTFE one. If the fluorination is further prolonged, decomposition of the sizing deteriorates the sizing film and forms non-adherent area, containing hydrophilic -COOH groups.

4 Conclusion

Direct fluorination with diluted F_2 gas (with N_2) at room temperature was applied to DGEBA-sized carbon fibres. Such operating conditions appear to be mild enough to avoid the total decomposition of the sizing. Moreover, SEM pictures, XRD and Raman analyses and tensile

tests on the fibres have shown that the treatment was not severe enough to modify or weaken the carbonaceous structure, considering chemical, structural or mechanical points of view. The covalent grafting of fluorine atoms on the sizing, with formation of CF, CF_2 and CF_3 bonds (by replacing C-OH, C-H, COC and C=C bonds of DGEBA), combined with an increase of the fibre roughening observed trough SEM, allows a hydrophobic behaviour of the fibre to be achieved. The optimal treatment has been found to be 20 minutes at room temperature with F_2/N_2 (50/50 vol %). Further fluorination leads to the formation of gaseous CF_4 and C_2F_6 and a sizing degradation, as seen through ^{19}F NMR with the drop of the amount of fluorinated species and the immediate water drop absorption for a 30-min fluorination. When controlled, the fluorination does not affect the mechanical properties of the sized fibres. The integration of these hydrophobic fluorinated fibres in a non-fluorinated (or fluorinated) epoxy is our next step, and could lead to a reduced moisture absorption compared to composites with non-fluorinated fibres, while keeping the same mechanical properties.

Acknowledgments

The authors wish to thank the Inorganic Material team of the Institut de Chimie de Clermont-Ferrand for their help during the experimental phase. This work was supported by SIGMA Clermont. SIGMA Clermont did not have any involvement in study design, in the collection, analysis and interpretation of data, in the writing of the report, or in the decision to submit the article for publication.

References

[1] S. Chand, 'Review Carbon fibers for composites', *J. Mater. Sci.*, vol. 35, pp. 1303–1313, 2000, doi: 10.1023/A:1004780301489.

[2] L. T. Drzal, 'The interphase in epoxy composites', in *Epoxy Resins and Composites II*, 1986, vol. 75, pp. 1–32, doi: 10.1007/BFb0017913.

[3] K. K. C. Ho, G. Beamson, G. Shia, N. V. Polyakova, and A. Bismarck, 'Surface and bulk properties of severely fluorinated carbon fibres', *J. Fluorine Chem.*, vol. 128, no. 11, pp. 1359–1368, Nov. 2007, doi: 10.1016/j.jfluchem.2007.06.005.

[4] J. D. H. Hughes, 'The carbon fibre/epoxy interface - A review', *Compos Sci Technol*, vol. 41, no. 1, pp. 13–45, Jan. 1991, doi: 10.1016/0266-3538(91)90050-Y.

[5] F. R. Jones, 'A Review of Interphase Formation and Design in Fibre-Reinforced Composites', *J Adhes Sci Technol*, vol. 24, no. 1, pp. 171–202, Jan. 2010, doi: 10.1163/016942409X12579497420609.

[6] R. L. Zhang, Y. D. Huang, L. Liu, Y. R. Tang, D. Su, and L. W. Xu, 'Effect of emulsifier content of sizing agent on the surface of carbon fibres and interface of its composites', *Appl. Surf. Sci.*, vol. 257, no. 8, pp. 3519–3523, Feb. 2011, doi: 10.1016/j.apsusc.2010.11.066.

[7] L. T. Drzal, M. J. Rich, and M. F. Koenig, 'Adhesion of Graphite Fibers to Epoxy Matrices. III. The Effect of Hygrothermal Exposure', *J Adhes*, vol. 18, no. 1, pp. 49–72, Jan. 1985, doi: 10.1080/00218468508074936.

[8] C. L. Arnold, D. Eyckens, L. Servinis, M. Nave, H. Yin, M. Ross, J. Pinson, B. Demir, T. Walsh and L. Henderson, 'Simultaneously increasing the hydrophobicity and interfacial adhesion of carbon fibres: a simple pathway to install passive functionality into composites', *J. Mater. Chem. A*, vol. 7, no. 22, pp. 13483–13494, 2019, doi: 10.1039/C9TA02436K.

[9] O. I. Gladunova, Yu. E. Fedorova, O. V. Astashkina, and A. A. Lysenko, 'Composites with Hydrophobic Surfaces', *Fibre Chem*, vol. 47, no. 4, pp. 317–319, Nov. 2015, doi: 10.1007/s10692-016-9686-5.

[10] B. Ameduri and H. Sawada, *Fluorinated Polymers: Volume 2: Applications*, vol. 2. Cambridge: Royal Society of Chemistry, 2016.

[11] L.-Y. Meng and S.-J. Park, 'Superhydrophobic carbon-based materials: a review of synthesis, structure, and applications', *Carbon lett.*, vol. 15, no. 2, pp. 89–104, Apr. 2014, doi: 10.5714/CL.2014.15.2.089.

[12] L. B. Boinovich and A. M. Emelyanenko, 'Hydrophobic materials and coatings: principles of design, properties and applications', *Russ. Chem. Rev.*, vol. 77, no. 7, pp. 583–600, Jul. 2008, doi: 10.1070/RC2008v077n07ABEH003775.

[13] J. Peyroux *et al.*, 'Surface modification of low-density polyethylene packaging film via direct fluorination', *Surf. Coat. Technol.*, vol. 292, pp. 144–154, Apr. 2016, doi: 10.1016/j.surfcoat.2016.03.021.

[14] A. P. Kharitonov and B. A. Loginov, 'Direct fluorination of polymer final products: From fundamental study to practical application', *Russ J Gen Chem*, vol. 79, no. 3, pp. 635–641, Mar. 2009, doi: 10.1134/S1070363209030451.

[15] A. P. Kharitonov, 'Improvement of Performance Characteristics of Polymer Materials by Direct Fluorination', *Chemistry for Sustainable Development*, vol. 12, pp. 625–630, 2004.

[16] A. P. Kharitonov and L. N. Kharitonova, 'Surface modification of polymers by direct fluorination: A convenient approach to improve commercial properties of polymeric articles', *Pure Appl. Chem.*, vol. 81, no. 3, pp. 451–471, Jan. 2009, doi: 10.1351/PAC-CON-08-06-02.

[17] A. P. Kharitonov, R. Taege, G. Ferrier, V. V. Teplyakov, D. A. Syrtsova, and G.-H. Koops, 'Direct fluorination - Useful tool to enhance commercial properties of polymer articles', *J. Fluorine Chem.*, vol. 126, no. 2, pp. 251–263, Feb. 2005, doi: 10.1016/j.jfluchem.2005.01.016.

[18] A. Bismarck *et al.*, 'Influence of fluorination on the properties of carbon fibres', *J. Fluorine Chem.*, vol. 84, no. 2, pp. 127–134, Sep. 1997, doi: 10.1016/S0022-1139(97)00029-8.

[19] K. K. C. Ho, A. F. Lee, and A. Bismarck, 'Fluorination of carbon fibres in atmospheric plasma', *Carbon*, vol. 45, no. 4, pp. 775–784, Apr. 2007, doi: 10.1016/j.carbon.2006.11.015.

[20] K. K. C. Ho, A. F. Lee, S. Lamoriniere, and A. Bismarck, 'Continuous atmospheric plasma fluorination of carbon fibres', *Compos. Part A Appl. Sci. Manuf.*, vol. 39, no. 2, pp. 364–373, Feb. 2008, doi: 10.1016/j.compositesa.2007.10.008.

[21] F. Saulnier, M. Dubois, K. Charlet, L. Frezet, and A. Beakou, 'Direct fluorination applied to wood flour used as a reinforcement for polymers', *Carbohydr. Polym.*, vol. 94, no. 1, pp. 642–646, Apr. 2013, doi: 10.1016/j.carbpol.2013.01.060.

[22] M. Pouzet, M. Dubois, K. Charlet, A. Béakou, J. M. Leban, and M. Baba, 'Fluorination renders the wood surface hydrophobic without any loss of physical and mechanical properties', *Ind Crops Prod*, vol. 133, pp. 133–141, Jul. 2019, doi: 10.1016/j.indcrop.2019.02.044.

[23] M. Pouzet, M. Dubois, K. Charlet, and A. Béakou, 'From hydrophilic to hydrophobic wood using direct fluorination: A localized treatment', *C R Chim*, vol. 21, no. 8, pp. 800–807, Aug. 2018, doi: 10.1016/j.crci.2018.03.009.

[24] M. Pouzet, D. Gautier, K. Charlet, M. Dubois, and A. Béakou, 'How to decrease the hydrophilicity of wood flour to process efficient composite materials', *Appl. Surf. Sci.*, vol. 353, pp. 1234–1241, Oct. 2015, doi: 10.1016/j.apsusc.2015.06.100.

[25] K. K. C. Ho, G. Kalinka, M. Q. Tran, N. V. Polyakova, and A. Bismarck, 'Fluorinated carbon fibres and their suitability as reinforcement for fluoropolymers', *Compos Sci Technol*, vol. 67, no. 13, pp. 2699–2706, Oct. 2007, doi: 10.1016/j.compscitech.2007.02.012.

[26] P. K. Mallick, *Fiber-Reinforced Composites: Materials, Manufacturing, and Design*, 3rd ed. CRC Press, 2007.

[27] M. Zayat, D. Davidov, and H. Selig, 'Fluorination of carbon fibers by halogen fluorides', *Carbon*, vol. 32, no. 3, pp. 485–491, 1994, doi: 10.1016/0008-6223(94)90170-8.

[28] V. Gupta, R. B. Mathur, O. P. Bahl, A. Tressaud, and S. Flandrois, 'Thermal stability of fluorine-intercalated carbon fibres', *Synth Met*, vol. 73, no. 1, pp. 69–75, Jul. 1995, doi: 10.1016/0379-6779(95)03299-1.

[29] R. B. Mathur, V. Gupta, O. P. Bahl, A. Tressaud, and S. Flandrois, 'Improvement in the mechanical properties of polyacrylonitrile (PAN)- based carbon fibers after fluorination', *Synth Met*, vol. 114, no. 2, pp. 197–200, 2000, doi: 10.1016/S0379-6779(00)00251-4.

[30] A. Tressaud *et al.*, 'Fluorine-intercalated carbon fibers - Structural and transport properties', *Carbon*, vol. 32, no. 8, pp. 1485–1492, 1994, doi: 10.1016/0008-6223(94)90143-0.

[31] W. Feng, P. Long, Y. Feng, and Y. Li, 'Two-Dimensional Fluorinated Graphene: Synthesis, Structures, Properties and Applications', *Adv. Sci.*, vol. 3, no. 7, p. 1500413, Jul. 2016, doi: 10.1002/advs.201500413.

[32] L. Fischer, U. Siemann, and W. Ruland, 'Structure and properties of fluorinated carbon fibers', *Colloid Polym Sci*, vol. 261, no. 9, pp. 744–749, Sep. 1983, doi: 10.1007/BF01410948.

[33] S.-J. Park, M.-K. Seo, and K.-Y. Rhee, ‘Studies on mechanical interfacial properties of oxy-fluorinated carbon fibers-reinforced composites’, *Mater. Sci. Eng. A*, vol. 356, no. 1–2, pp. 219–226, Sep. 2003, doi: 10.1016/S0921-5093(03)00134-5.

[34] A. P. Kharitonov, ‘Direct fluorination of polymers - From fundamental research to industrial applications’, *Prog. Org. Coat.*, vol. 61, no. 2–4, pp. 192–204, Feb. 2008, doi: 10.1016/j.porgcoat.2007.09.027.

[35] A. P. Kharitonov, ‘Practical applications of the direct fluorination of polymers’, *J. Fluorine Chem.*, vol. 103, pp. 123–127, 2000, doi: 10.1016/S0022-1139(99)00312-7.

[36] Z. Dai, F. Shi, B. Zhang, M. Li, and Z. Zhang, ‘Effect of sizing on carbon fiber surface properties and fibers/epoxy interfacial adhesion’, *Appl. Surf. Sci.*, vol. 257, no. 15, pp. 6980–6985, May 2011, doi: 10.1016/j.apsusc.2011.03.047.

[37] S. R. Taylor, ‘Coatings for Corrosion Protection: Inorganic’, in *Encyclopedia of Materials: Science and Technology*, Elsevier, 2001, pp. 1263–1269.

[38] B. Janczuk and A. Zdziennicka, ‘A study on the components of surface free energy of quartz from contact angle measurements’, *J. Mater. Sci.*, vol. 29, no. 13, pp. 3559–3564, Jul. 1994, doi: 10.1007/BF00352063.

[39] K. Charlet, S. Eve, J. P. Jernot, M. Gomina, and J. Breard, ‘Tensile deformation of a flax fiber’, *Procedia Eng.*, vol. 1, no. 1, pp. 233–236, Jul. 2009, doi: 10.1016/j.proeng.2009.06.055.

[40] A. Roudier *et al.*, ‘Caractérisation des propriétés biochimiques et hygroscopiques d’une fibre de lin’, *Matériaux & Techniques*, vol. 100, no. 5, pp. 525–535, 2012, doi: 10.1051/mattech/2012044.

[41] I. Kruppke, C. Scheffler, F. Simon, R.-D. Hund, and C. Cherif, ‘Surface Treatment of Carbon Fibers by Oxy-Fluorination’, *Materials*, vol. 12, no. 4, p. 18, Feb. 2019, doi: 10.3390/ma12040565.

[42] Z. Q. Li, C. J. Lu, Z. P. Xia, Y. Zhou, and Z. Luo, ‘X-ray diffraction patterns of graphite and turbostratic carbon’, *Carbon*, vol. 45, no. 8, pp. 1686–1695, Jul. 2007, doi: 10.1016/j.carbon.2007.03.038.

[43] M. Rodriguez-Garcia, S. Londoño-Restrepo, C. Ramirez-Guttierez, and B. Millan-Malo, ‘Effect of the crystal size on the X-ray diffraction patterns of isolated orthorhombic starches: A-type’, *Preprint*, 2019, [Online]. Available: https://arxiv.org/abs/1808.02966.

[44] J. I. Langford and A. J. C. Wilson, ‘Scherrer after Sixty Years: A Survey and Some New Results in the Determination of Crystallite Size’, *J. Appl. Cryst.*, pp. 102–113, 1978, doi: 10.1107/S0021889878012844.

[45] B. D. Cullity and S. R. Stock, *Elements of X-ray diffraction*, 3rd ed. Pearson/Prentice Hall, 2001.

[46] O. Paris, Ed., *Structure and Multiscale Mechanics of Carbon Nanomaterials*, vol. 563. Springer Vienna, 2016.

[47] D. D. L. Chung, *Carbon fiber composites*. Butterworth-Heinemann, 1994.

[48] G. A. Zickler, B. Smarsly, N. Gierlinger, H. Peterlik, and O. Paris, ‘A reconsideration of the relationship between the crystallite size La of carbons determined by X-ray diffraction and Raman spectroscopy’, *Carbon*, vol. 44, no. 15, pp. 3239–3246, Dec. 2006, doi: 10.1016/j.carbon.2006.06.029.

[49] C. Pardanaud, C. Martin, and P. Roubin, 'Multiwavelength Raman spectroscopy analysis of a large sampling of disordered carbons extracted from the Tore Supra tokamak', *Vib Spectrosc*, vol. 70, pp. 187–192, Jan. 2014, doi: 10.1016/j.vibspec.2013.12.004.

[50] C. Sisu, R. Iordanescu, V. Stanciu, I. Stefanescu, A. M. Vlaicu, and V. V. Grecu, 'Raman Spectroscopy Studies of some Carbon Molecular Sieves', *Dig. J. Nanomater. Biostructures*, vol. 11, no. 2, pp. 435–442, 2016.

[51] S. Surblé *et al.*, 'Complementary Ion Beam Analysis and Raman Studies for Investigation of the Carbon Coating Impact on Li Insertion/Deinsertion Process at LiFePO4/C Electrodes', *J. Electrochem. Soc.*, vol. 164, no. 14, pp. A3538–A3544, 2017, doi: 10.1149/2.0471714jes.

[52] A. C. Ferrari and J. Robertson, 'Interpretation of Raman spectra of disordered and amorphous carbon', *Phys. Rev. B*, vol. 61, no. 20, pp. 14095–14107, May 2000, doi: 10.1103/PhysRevB.61.14095.

[53] A. Merlen, J. Buijnsters, and C. Pardanaud, 'A Guide to and Review of the Use of Multiwavelength Raman Spectroscopy for Characterizing Defective Aromatic Carbon Solids: from Graphene to Amorphous Carbons', *Coatings*, vol. 7, no. 10, p. 153, Sep. 2017, doi: 10.3390/coatings7100153.

[54] A. C. Ferrari and J. Robertson, 'Raman spectroscopy of amorphous, nanostructured, diamond–like carbon, and nanodiamond', *Philos Trans A Math Phys Eng Sci*, vol. 362, no. 1824, pp. 2477–2512, Nov. 2004, doi: 10.1098/rsta.2004.1452.

[55] V. H. Dalvi and P. J. Rossky, 'Molecular origins of fluorocarbon hydrophobicity', *Proc. Natl. Acad. Sci. U.S.A.*, vol. 107, no. 31, pp. 13603–13607, Aug. 2010, doi: 10.1073/pnas.0915169107.

[56] M. K. Bernett and W. A. Zisman, 'Relation of Wettability by Aqueous Solutions to the Surface Constitution of Low-energy Solids', *J. Phys. Chem.*, vol. 63, no. 8, pp. 1241–1246, Aug. 1959, doi: 10.1021/j150578a006.

[57] A. P. Kharitonov, G. V. Simbirtseva, A. Tressaud, E. Durand, C. Labrugère, and M. Dubois, 'Comparison of the surface modifications of polymers induced by direct fluorination and rf-plasma using fluorinated gases', *J. Fluorine Chem.*, vol. 165, pp. 49–60, Sep. 2014, doi: 10.1016/j.jfluchem.2014.05.002.

[58] F. J. du Toit and R. D. Sanderson, 'Surface fluorination of polypropylene', *J. Fluorine Chem.*, vol. 98, no. 2, pp. 107–114, Sep. 1999, doi: 10.1016/S0022-1139(99)00091-3.

[59] D. K. Owens and R. C. Wendt, 'Estimation of the surface free energy of polymers', *J. Appl. Polym. Sci.*, vol. 13, no. 8, pp. 1741–1747, Aug. 1969, doi: 10.1002/app.1969.070130815.

[60] K. Song, J. Lee, S.-O. Choi, and J. Kim, 'Interaction of Surface Energy Components between Solid and Liquid on Wettability, and Its Application to Textile Anti-Wetting Finish', *Polymers*, vol. 11, no. 3, p. 498, Mar. 2019, doi: 10.3390/polym11030498.

[61] S. Cholake, M. Mada, R. K. Singh Raman, Y. Bai, XL Zhao, S. Rizkalla, and S. Bandyopadhyay 'Quantitative Analysis of Curing Mechanisms of Epoxy Resin by Mid- and Near- Fourier Transform Infra Red Spectroscopy', *Def Sci J*, vol. 64, no. 3, pp. 314–321, May 2014, doi: 10.14429/dsj.64.7326.

[62] M. G. González, J. C. Cabanelas, and J. Baselga, 'Applications of FTIR on Epoxy Resins - Identification, Monitoring the Curing Process, Phase Separation and Water

Uptake', in *Infrared Spectroscopy - Materials Science, Engineering and Technology*, T. Theophanides, Ed. InTech, 2012.

[63] F. Delor-Jestin, D. Drouin, P.-Y. Cheval, and J. Lacoste, 'Thermal and photochemical ageing of epoxy resin – Influence of curing agents', *Polym. Degrad. Stab.*, vol. 91, no. 6, pp. 1247–1255, Jun. 2006, doi: 10.1016/j.polymdegradstab.2005.09.009.

[64] A. Cherdoud-Chihani, M. Mouzali, and M. J. M. Abadie, 'Study of crosslinking acid copolymer/DGEBA systems by FTIR', *J. Appl. Polym. Sci.*, vol. 87, no. 13, pp. 2033–2051, Mar. 2003, doi: 10.1002/app.11389.

[65] E. Sharmin, M. S. Alam, R. K. Philip, and S. Ahmad, 'Linseed amide diol/DGEBA epoxy blends for coating applications: Preparation, characterization, ageing studies and coating properties', *Prog. Org. Coat.*, vol. 67, no. 2, pp. 170–179, Feb. 2010, doi: 10.1016/j.porgcoat.2009.09.012.

[66] Y. Ngono and Y. Marechal, 'Epoxy-amine reticulates observed by infrared spectrometry. II. Modifications of structure and of hydration abilities after irradiation in a dry atmosphere', *J. Polym. Sci. Pol. Phys.*, vol. 38, no. 2, pp. 329–340, 2000, doi: 10.1002/(SICI)1099-0488(20000115)38:2<329::AID-POLB5>3.0.CO;2-T.

[67] Y. Zahra, 'Dégradation de réseaux époxy-amine en ambiance nucléaire', Ecole Nationale Supérieure des Arts et Métiers, France, 2012.

[68] A. P. Kharitonov, R. Taege, G. Ferrier, and N. P. Piven, 'The kinetics and mechanism of the direct fluorination of polyethylenes', *Surf. Coat. Int. B: Coat. Trans.*, vol. 88, no. 3, pp. 201–212, Sep. 2005, doi: 10.1007/BF02699574.

[69] M. Pouzet, M. Dubois, K. Charlet, E. Petit, A. Béakou, and C. Dupont, 'Fluorination/Torrefaction Combination to Further Improve the Hydrophobicity of Wood', *Macromol. Chem. Phys.*, vol. 220, no. 14, p. 1900041, Jul. 2019, doi: 10.1002/macp.201900041.

[70] N. S. Broyles, R. Chan, R. M. Davis, J. J. Lesko, and J. S. Riffle, 'Sizing of carbon fibres with aqueous solutions of poly(vinyl pyrollidone)', *Polymer*, vol. 39, no. 12, pp. 2607–2613, 1998, doi: 10.1016/S0032-3861(97)00562-4.

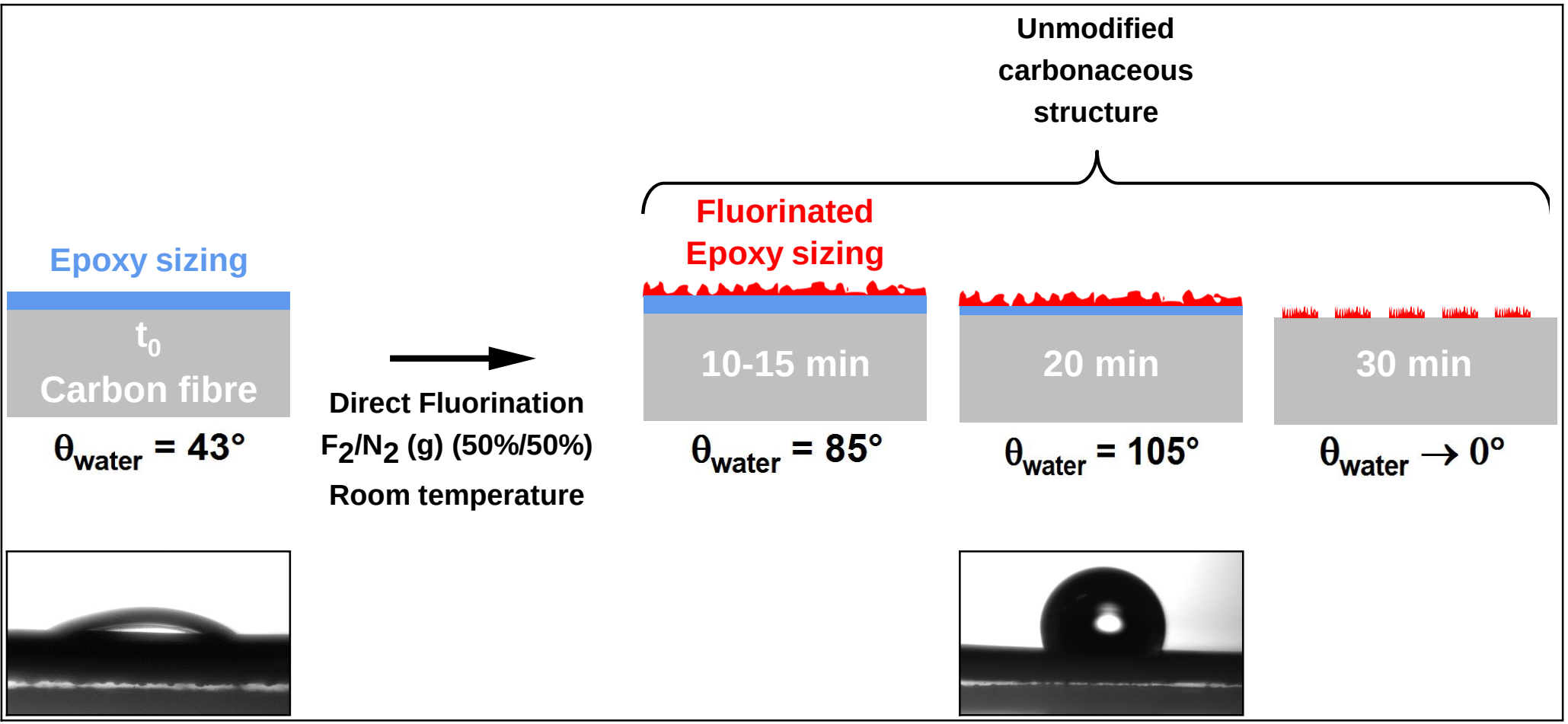
Unmodified
carbonaceous
structure
Epoxy sizing
t_0
Carbon fibre
θ_{water} = 43°
Direct Fluorination
F_2/N_2 (g) (50%/50%)
Room temperature
Fluorinated
Epoxy sizing
10-15 min
θ_{water} = 85°
20 min
θ_{water} = 105°
30 min
$\theta_{water} \rightarrow 0°$